GUIDELINES FOR IFOC DRIVES COMMISSIONING

R. Reginatto A. S. Bazanella

Department of Electrical Engineering, Universidade Federal do Rio Grande do Sul
Av. Osvaldo Aranha 103, 90035-190, Porto Alegre, RS, Brazil
romeu@eletro.ufrgs.br, bazanela@eletro.ufrgs.br

Abstract— In this paper we provide guidelines for the comissioning of induction motor drives based on indirect field oriented control. We rely on robust stability results for IFOC drives to provide such guidelines. In doing so, we aim at a comissioning that is robust against practical rotor time constant mismatches and practical operating conditions. The guidelines are valid for both speed control with a PI regulator and position control with a PD regulator.

Key Words— Indirect field oriented control; induction motors; commissioning

1 Introduction

Indirect Field Oriented Control (IFOC) is a well established and widely applied control technique when dealing with high performance induction motor drives (Novotny and Lorenz, 1986; Leonhard, 1985; Bose, 1987). The commissioning of an IFOC requires the knowledge of the rotor time constant, a parameter that can vary widely in practice (Krishnan and Doran, 1987; Marino et al., 1993) and is known to cause performance and stability problems. Most results in the literature address this problem from the application point of view focusing on the performance issue without providing stability guarantees. Only the recent works (Bazanella and Reginatto, 2000; Bazanella et al., 1999; Ortega et al., 1996; De Wit et al., 1996) have aimed at filling in this gap by providing IFOC with a firm theoretical foundation.

It has been shown that the speed control of induction motors through IFOC is globally asymptotically stable for any constant load torque if the rotor time constant is perfectly known or the error in its estimation is sufficiently small (De Wit et al., 1996; Bazanella and Reginatto, 2000). In a previous paper (Bazanella and Reginatto, 2000) we also showed that saddle-node bifurcations occur for certain values of the mismatch in this estimation and certain load conditions. Another possible mechanism for loss of stability, namely, the occurrence of Hopf bifurcations, has been considered in (Bazanella and Reginatto, 2001; Bazanella et al., 1999; De Wit et al., 1996; Espinosa-Perez et al., 1998). Contrary to saddle-node bifurcations, this mechanism of loss of stability depends on the settings of the speed control loop (De Wit et al., 1996; Espinosa-Perez et al., 1998; Bazanella et al., 1999). In the recent works (Reginatto and Bazanella, 2000; Bazanella et al., 2000), effective results have been provided to analyze the global asymptotic stability property of IFOC drives. Also in this case, the setting of the PI speed loop controller plays a fundamental role on the size of the region on the parameter space where the IFOC drives exhibits this important property.

This set of results elucidate the influence of all relevant tunable parameters in an IFOC drive on its stability properties. On the base of these results, we will provide useful guidelines for the setting of such parameters in the commissioning of any IFOC drive. The guidelines are intended for a design that keeps all possible instability mechanisms far enough from a practical operating region in the parameter space.

The paper is organizes as follows. In Section 2 the system modeling and the control equations are given and some additional convenient notation and concepts are introduced. The mechanisms of loss of local stability are clarified in Section 3. Based on these results, in Section 4 we derive guidelines for setting the estimate of the rotor time constant and the parameters of the PI speed controller in order to guarantee stability of the system for practical parameter mismatches. A case study is presented in Section 5.

2 Modeling

We consider the indirect field oriented control (IFOC) of induction motor drives. Field oriented control is usually employed as a means to achieve high performance transient response in speed, position, or torque control. The implementation of IFOC employs stator current control, i.e., the induction machine is current fed, and allows three control inputs, namely: i_{ds}, the direct axis stator current component; i_{qs}, the quadrature axis stator current component; and ω_{sl}, the slip frequency (Novotny and Lorenz, 1986; Leonhard, 1985).

IFOC consists in setting ω_{sl} and a specific initialization procedure in the attempt to achieve a control decoupling between i_{ds} and i_{qs}, the first acting on the rotor flux level, while the later acting on the developed torque. More specifically, we have (Novotny and Lorenz, 1986; De Wit

et al., 1996):

$$\omega_{sl} = \hat{c}_1 \frac{i_{qs}}{i_{ds}} \tag{1}$$

$$i_{ds} = u_2^0 \tag{2}$$

where $\hat{c}_1$ is an estimate for the inverse rotor time constant $c_1 = \frac{L_r}{R_r}$, L_r being the rotor inductance and R_r the rotor resistance, and u_2^0 is some constant which defines the rotor flux level.

In speed regulation applications, usually a PI regulator is used to act on the remaining control input i_{qs},

$$i_{qs} = k_p e_w + k_i \int_0^t e_w(\zeta)\, d\zeta \tag{3}$$

where k_p and k_i are the gains of the PI speed controller and $e_w = w_{ref} - w$ is the rotor speed error - the difference between the constant reference velocity the actual rotor speed.

The rotor time constant is a critical parameter for IFOC. If $\hat{c}_1 = c_1$, that is, if we have a perfect estimate of the rotor time constant, we say that the control is tuned, otherwise it is said to be detuned. Accordingly, we define

$$\kappa \triangleq \frac{\hat{c}_1}{c_1} \tag{4}$$

as the degree of tuning. It is clear that $\kappa > 0$ and the control is tuned if and only if $\kappa = 1$.

By choosing state variables $[x_1,\ x_2,\ x_3,\ x_4] = [\lambda_{qr},\ \lambda_{dr},\ e_w,\ i_{qs}]$, we obtain the induction motor model under field oriented control (1)-(2) and PI speed regulation (3) described as:

$$\dot{x}_1 = -c_1 x_1 + c_2 x_4 - \frac{\kappa c_1}{u_2^0} x_2 x_4 \tag{5}$$

$$\dot{x}_2 = -c_1 x_2 + c_2 u_2^0 + \frac{\kappa c_1}{u_2^0} x_1 x_4 \tag{6}$$

$$\dot{x}_3 = -c_3 x_3 - c_4[c_5(x_2 x_4 - u_2^0 x_1) - T_e] \tag{7}$$

$$\dot{x}_4 = k_c x_3 - k_p c_4[c_5(x_2 x_4 - u_2^0 x_1) - T_e] \tag{8}$$

where λ_{qr} and λ_{dr} stand for the quadrature and direct axis components of the rotor flux; T_m is the load torque, which is assumed constant; c_1 to c_6 are machine parameters; and we have defined $k_c \triangleq k_i - k_p c_3$ and $T_e \triangleq T_m + \frac{c_3}{c_4} w_{ref}$.

It is easy to show that for position regulation with a proportional-derivative controller the same model is obtained after a change of variables, so that all the results derived for speed regulation are also valid for position regulation.

2.1 The tuned system

A constant rotor flux must be established inside the motor before the systems can be operated. This is called the fluxification phase of IFOC, and is achieved by setting $i_{ds} = u_2^0$ and $w_{ref} = 0$ with the motor in stand-still condition. The steady-state reached under these conditions is given by $x = x^o = [0,\ \frac{c_2}{c_1} u_2^0,\ 0,\ 0]'$, which is considered the initial state for IFOC operation.

In the tuned case, $\kappa = 1$, the model (5)-(8) simplifies considerably. First, notice that starting from $x(0) = x^o$, the fluxes x_1 and x_2 remain constant for all times, regardless of the behavior of x_4. Now, taking this into account, the remaining equations (7)-(8) can be rearranged as

$$\begin{bmatrix} \dot{x}_3 \\ \dot{x}_4 \end{bmatrix} = \begin{bmatrix} -c_3 & -\frac{c_4 c_5 c_2 u_2^0}{c_1} \\ (k_i - k_p c_3) & -\frac{k_p c_4 c_5 c_2 u_2^0}{c_1} \end{bmatrix} \begin{bmatrix} x_3 \\ x_4 \end{bmatrix} + \begin{bmatrix} c_3 & c_4 \\ k_p c_3 & k_p c_4 \end{bmatrix} \begin{bmatrix} w_{ref} \\ T_m \end{bmatrix} \tag{9}$$

which is a second-order *linear* system. We shall refer to the dynamic system (9) as the *tuned system*, which is usually taken as a base for setting the PI gains. A block-diagram of the tuned system is given in Figure 1, where the plant is the induction motor under perfect field-orientation (tuned).

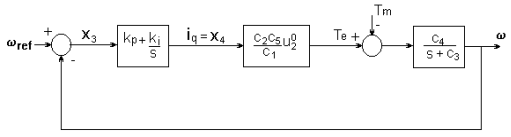

Figure 1. Block diagram of the tuned system.

The tuned system just defined represents an ideal situation, in which perfect field-orientation is achieved. Under this condition optimal performance can be achieved, and the PI speed controller is set for the desired performance. Since in this case the controlled system is linear and of order two, the tuning of the PI controller under the assumption of perfect field-orientation is simple, and in theory arbitrary performance can be achieved.

From (9), the closed-loop eigenvalues are the roots of the characteristic polynomial

$$p_T(\lambda) = \lambda^2 + (c_3 + k_p K)\lambda + k_i K \tag{10}$$

where $K \triangleq \frac{c_2 c_4 c_5 u_2^0}{c_1}$. Then the PI parameters k_p and k_i can be chosen to arbitrarily assign the closed-loop eigenvalues of the tuned system. Indeed, let the desired closed-loop characteristic (Hurwitz) polynomial be written as

$$\lambda^2 + a_1 \lambda + a_0, \quad a_0 > 0,\ a_1 > 0 \tag{11}$$

Then, equating the coefficients in (10) and (11) yields

$$k_p = \frac{a_1 - c_3}{K}, \quad k_i = \frac{a_0}{K} \tag{12}$$

Once the closed-loop poles are chosen the parameters k_p and k_i can be calculated from (12).

3 Mechanisms of loss of stability

Let us define the dimensionless variables $r \triangleq \frac{x_4^e}{u_2^0}$ and $r^* \triangleq \frac{T_e c_1}{c_5 c_2 (u_2^0)^2}$. The constant r^* represents the system loading, since it is proportional to the electrical torque developed in steady-state. The parameter r can be shown to satisfy the third-order polynomial equation (Bazanella and Reginatto, 2000)

$$\kappa r^3 - r^* \kappa^2 r^2 + \kappa r - r^* = 0 \tag{13}$$

and the equilibria can be written as

$$\begin{bmatrix} x_1^e \\ x_2^e \\ x_3^e \\ x_4^e \end{bmatrix} = \begin{bmatrix} \frac{c_2 u_2^0}{c_1} \frac{1-\kappa}{1+\kappa^2 r^2} r \\ \frac{c_2 u_2^0}{c_1} \frac{1+\kappa r^2}{1+\kappa^2 r^2} \\ 0 \\ u_2^0 \; r \end{bmatrix} \tag{14}$$

The equilibrium is then parameterized in terms of a single dimensionless quantity r, which satisfies equation (13). This is a third order polynomial equation whose coefficients are also dimensionless and depend only on the degree of tuning κ and the normalized load as denoted by r^*.

The complete characterization of the equilibria is illustrated in Figure 2 (Bazanella and Reginatto, 2000). The two curves, on the (κ, r^*) parameter space, delimit the region where equation (13) has 3 real solutions (3 equilibrium points). For any point outside the region we have a unique equilibrium point. The point where the two curves intersect is $\kappa = 3$, $r^* = \frac{\sqrt{3}}{3}$. Thus, we have a unique equilibrium point for any load condition if and only if $\kappa < 3$.

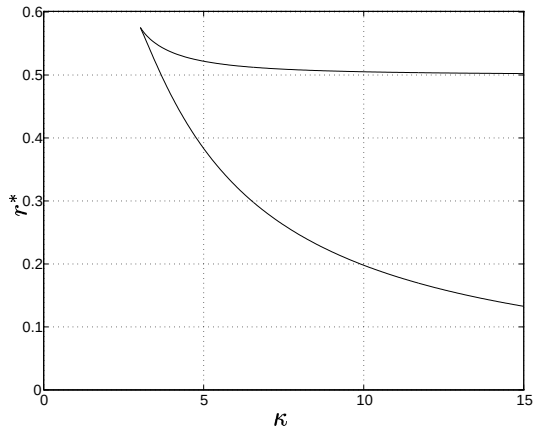

Figure 2. Locus of the points in the parameter space where the number of equilibria changes.

It has also been shown (Bazanella and Reginatto, 2000; De Wit et al., 1996) that the equilibrium is globally asymptotically stable in the tuned condition. Hence, for the tuned condition the Jacobian of (5)-(8) has all its eigenvalues in the open left half plane. As the parameters κ and r^* vary, loss of stability can be detected by looking at the eigenvalues of the Jacobian, as either a pair of complex eigenvalues or a single real eigenvalue cross the imaginary axis towards the right half plane. If a real eigenvalue crosses the imaginary axis through zero then a saddle-node bifurcation takes place. It has been shown in (Bazanella and Reginatto, 2000) that a saddle-node bifurcation occurs at the points the number of equilibria changes. Then, in the region inside the two curves in Figure 2 the systems has one unstable equilibrium point, regardless of the PI setting.

3.1 Hopf bifurcations

A Hopf bifurcation characterizes an equilibrium becoming unstable by the crossing of the $j\omega$ axis by two complex conjugate eigenvalues of the jacobian. In the important case of zero load operation, a closed form condition for existence of Hopf bifurcations can be derived from as follows (Bazanella et al., 1999; Bazanella and Reginatto, 2001).

Lemma 1 *Let $c_3 \equiv 0$ and $T_m \equiv 0$. Then, no Hopf bifurcation takes place for any $\kappa > 0$ provided that a_0, a_1 satisfy the relation*

$$a_0 \leq a_1(c_1 + a_1) \tag{15}$$

If condition 15 is not satisfied, then a Hopf bifurcation takes place at

$$\kappa = \kappa_h \triangleq \frac{a_0(c_1 + a_1)}{c_1(a_0 - a_1(c_1 + a_1))} \tag{16}$$

◊

Condition (15) is satisfied whenever the closed-loop eigenvalues for the tuned system are chosen to be real. If complex closed-loop eigenvalues are desired, then the imaginary part has to be chosen sufficiently small in order to satisfy (15). Figure 3 illustrates the situation for the complex eigenvalues case, i.e., $\lambda_{1,2} = -\sigma \pm j\omega$. The value of κ_h is plotted as a function of σ/c_1 and $j\omega/c_1$, the normalized real and imaginary part of the chosen eigenvalues for the tuned system, respectively. The figure also shows the region, in the $(\sigma, j\omega)$ plane, where no Hopf bifurcation takes place for any κ. We can see that κ_h approaches ∞ at the boundary of that region and rapidly decreases to practical values as the damping is decreased.

In order to obtain a better insight into the occurrence of Hopf bifurcation and its relation to the PI setting, we choose to parameterize the PI gains in terms of the eigenvalues of the tuned system, normalized to the inverse of the rotor time constant. From the zero-load case we can see a major influence of the eigenvalues being chosen real or complex. We will then consider two cases:

1. The eigenvalues of the tuned system are both real and equal to $-\eta c_1$, where η is a new dimensionless parameter. Then $a_1 =$

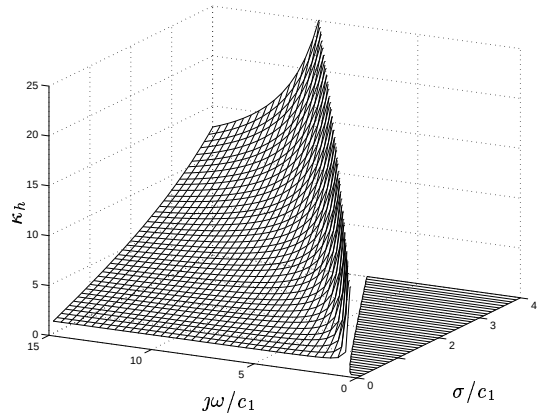

Figure 3. Parameter chart for the zero load case. Tuned system eigenvalues $\lambda_{1,2} = -\sigma \pm j\omega$. The dashed region in the $(\sigma, j\omega)$ plane illustrates the region where no Hopf bifurcation takes place for any κ.

$2\eta c_1$ and $a_0 = \eta^2.c_1^2$. This case is of major interest since even for the zero-load case, complex eigenvalues lead to the occurrence of Hopf bifurcation for certain values of κ. Moreover, oscillatory responses are usually not desirable for the IFOC drive.

2. The eigenvalues of the tuned system are chosen for a critically damped response, i.e., equal to $-\eta c_1(1 \pm j)$. Then $a_1 = 2\eta c_1$ and $a_0 = 2\eta^2.c_1^2$. Besides completing the identification of the effect of complex eigenvalues on the Hopf bifurcation in the presence of load, this case might be of interest in application for which a lower rise-time is more important than no overshoot.

With the PI gains parameterized in terms of the dimensionless parameter η, we can proceed to study the occurrence of Hopf bifurcations with respect to three parameters (κ, r^*, η). We have the following result (Bazanella and Reginatto, 2001; Bazanella et al., 1999)

Proposition 1 *Let λ_1, λ_2 denote the eigenvalues of the tuned system (9) with $c_3 = 0$ and choose the PI settings such that $\lambda_1 = \lambda_2 = -\eta.c_1$. Under these conditions the equilibrium of the system (5)-(8) is locally asymptotically stable for all $(\kappa, r^*) \in \mathcal{D}^* \triangleq \{(0,3] \times [0,2]\}$ if $\eta < 23$.* $\Diamond$

Then robust stability of the IFOC out of the tuning condition is guaranteed by proper assignment of the dynamics of the tuned system. Robust stability is guaranteed if the tuned system is designed to be non oscillatory and not faster than 23 times the inverse of the rotor time constant.

Figure 4 shows the bifurcation curves for the three different choices of the closed-loop eigenvalues: $\eta = 15$, $\eta = 23$ and $\eta = 30$. Each curve represents the locus of the points at which a Hopf bifurcation occurs for each different PI setting. For each setting, the system is locally stable outside the corresponding curve and unstable inside it. If the eigenvalues are moved too far away towards the left, the bifurcation tends to occur for lower values of κ.

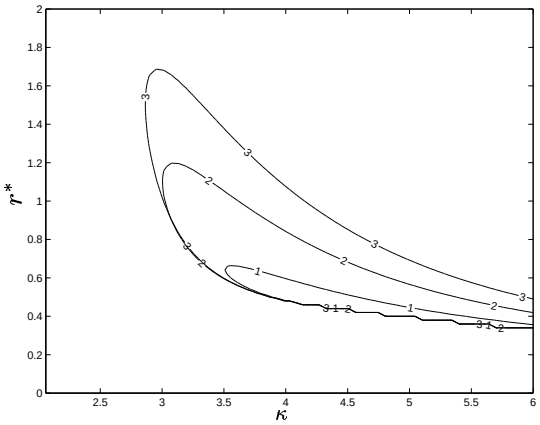

Figure 4. Hopf bifurcation for: $\lambda_{1,2} = -15c_1$ (1), $\lambda_{1,2} = -23c_1$ (2), $\lambda_1 = \lambda_2 = -30c_1$ (3).

Figure 5 shows the bifurcation curves for three choices of critically damped closed-loop eigenvalues. By comparing it with Figure 4, we can see that the Hopf bifurcation occurs at lower values of κ in this case. Moreover, the instability domain (region inside the curves) is considerably larger.

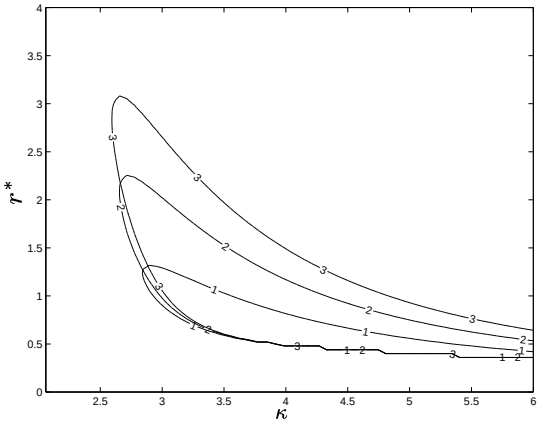

Figure 5. Hopf bifurcation for: $\lambda_{1,2} = -15c_1(1 \pm j)$ (1), $\lambda_{1,2} = -23c_1(1 \pm j)$ (2), $\lambda_1 = \lambda_2 = -30c_1(1 \pm j)$ (3).

4 Discussion on guidelines for commissioning

4.1 Setting of $\hat{c}_1$

The parameter c_1 stands for the inverse of the rotor time constant, i.e., $c_1 = \frac{R_r}{L_r}$. Thus, considering that L_r is constant, we obtain

$$\kappa = \frac{\hat{R}_r}{R_r} \tag{17}$$

where $\hat{R}_r$ is the estimated value of the actual rotor resistance R_r.

The rotor resistance is known to vary widely according to the rotor temperature. In most cases, temperature variations inside the rotor can cause the rotor time constant to vary more than 50% but not more than 100% (Krishnan and Doran, 1987). Hence, $0.5 < \kappa < 2$ in most practical cases.

The setting of $\hat{R}_r$ smaller than R_r leads to $\kappa < 1$. In this case, local stability is guaranteed, since neither saddle-node bifurcation nor Hopf bifurcations take place for reasonable designs of the PI controller. On the other hand, this region is also characterized by an increasing of the rotor flux with respect to its value in the tuned condition. Thus $\kappa < 1$ tends to cause flux saturation inside the motor, thus increasing core losses.

On the other hand, by setting $\hat{R}_r$ larger than R_r we cause the motor to operate with $\kappa > 1$. We know that in this region either saddle-node or Hopf bifurcation may occur. Saddle-node bifurcations occur for $\kappa > 3$, regardless of the PI setting. Hopf bifurcation, on the other hand, depend on the PI setting and may occur even for values of $\kappa < 3$. Thus, the operation in this region is not advisable for an IFOC drive.

Based on this discussion we can propose the following procedure to set the parameter $\hat{R}_r$.

1. Obtain a measure of R_r, say $\hat{R}_r^c$, with the motor cold;
2. Obtain $\hat{R}_r^h = 2\hat{R}_r^c$, an estimate of the value of R_r with the motor hot;
3. Set $\hat{R}_r = \frac{\hat{R}_r^c + \hat{R}_r^h}{2}$.

With this procedure, the values of κ are expected to be in the interval $0.75 \leq \kappa \leq 1.5$, in which local stability is guaranteed for reasonable PI settings. The procedure can also be started by measuring $\hat{R}_r^h$ and then estimating $\hat{R}_r^c = \hat{R}_r^h/2$.

4.2 Setting of the PI gains

The design of the PI controller is usually based on the tuned system only, thereby disregarding uncertainties in the rotor time constant. We have seen that, in most cases temperature variations inside the rotor can cause the rotor time constant from 50% to 100% (Krishnan and Doran, 1987). Moreover, in section 4.1 we provided a procedure to set $\hat{c}_1$ so that to keep κ close to the interval [0.75, 1.5].

Although stability is only lost through the occurrence of a bifurcation, a nearby bifurcation is enough to cause unsatisfactory transient behavior. Thus, considering that the procedure for setting $\hat{c}_1$ has been applied, it is reasonable to think of a PI setting that would avoid Hopf bifurcations to take place for $\kappa \in (0,\ 3]$. We cannot pursue anything larger than that, since for $\kappa > 3$ there always exist a range for r^* for which an unstable equilibrium point exists, regardless of the PI settings (Bazanella and Reginatto, 2000) (see Figure 2).

In analyzing the occurrence of Hopf bifurcation, we also have to consider the effect of the normalized load r^*. It is simple to verify that r^* coincides with the ratio x_4^e/u_2^0 for tuned operation. In general, this ratio is no larger than 2, so we concentrate on a range for r^* given by $0 \leq r^* \leq 2$.

Taking these considerations into account, we choose to search for PI settings that will avoid Hopf bifurcations in the domain $(\kappa,\ r^*) \in \mathcal{D}^* \triangleq \{(0, 3] \times [0, 2]\}$.

Poor PI setting can cause Hopf bifurcations basically in two different ways. One is to make the closed-loop response oscillatory by assigning complex conjugate eigenvalues with low damping. The second one is to force the closed-loop response to be very fast by choosing the closed-loop eigenvalues too far away to the left in the complex plane.

Following the statement of Proposition 1, Hopf bifurcations can be avoided for all parameters in the region $\mathcal{D}^*$ by setting the PI gains so that the closed-loop poles of the tuned system are $\lambda_1 = \lambda_2 = -\eta.c_1$ with $0 < \eta < 23$. This setting of the tuned system allows enough freedom to accommodate for the desired transient performance. Most of the IFOC drives exhibit satisfactory transient performance for η no larger than 10.

The choice of complex eigenvalues for the tuned system, although possibly of interest for some application, is a bad choice from the robustness point of view. We can verify in Figure 4 and 5 that the lower the damping, the lower the value of κ for which a Hopf bifurcation occurs. Thus, when commissioning an IFOC drive with this property, one has to be aware of its implications on the robustness of the drive.

The choice of real eigenvalues with small η for the tuned system is also adequate for global asymptotic stability. This fact has been observed in (Reginatto and Bazanella, 2000), where it was shown that the region in the parameter space $(\kappa,\ r^*)$ for which global asymptotic stability can be guaranteed shrinks when η is increased.

Based on this analysis we can propose as a guideline for setting the PI gains the following: chose real closed-loop poles for the tuned system with the smallest possible η that yields the desired transient performance. Avoid using η larger than 10 in order to keep the bifurcation far away, thus improving robustness.

5 Transient performance

In order to illustrate the effects of Hopf bifurcations on the system's performance, we present some simulations for a real 1 HP squirrel-cage induction motor with the following parameters:

$c_1 = 13.67\ s^{-1}$, $c_2 = 1.56\ H.s^{-1}$, $c_3 = 0.59s^{-1}$, $c_4 = 1,176kg^{-1}m^{-2}$, $c_5 = 2.86$ and $u_2^0 = 4\ A$.

Figure 6 shows the system response to several steps of load torque, starting from no load until the system reaches a Hopf bifurcation. The load torque variation is chosen in accordance with the r^* step variation in Figure 6. The eigenvalues of the tuned system were chosen $\lambda_{1,2} = (-1.2 \pm j7)c_1$. It is clear that the dynamic performance of the system is deteriorated as it approaches the bifurcation, becoming very poor much before reaching it. After the bifurcation occurs, a sustained oscillation is observed.

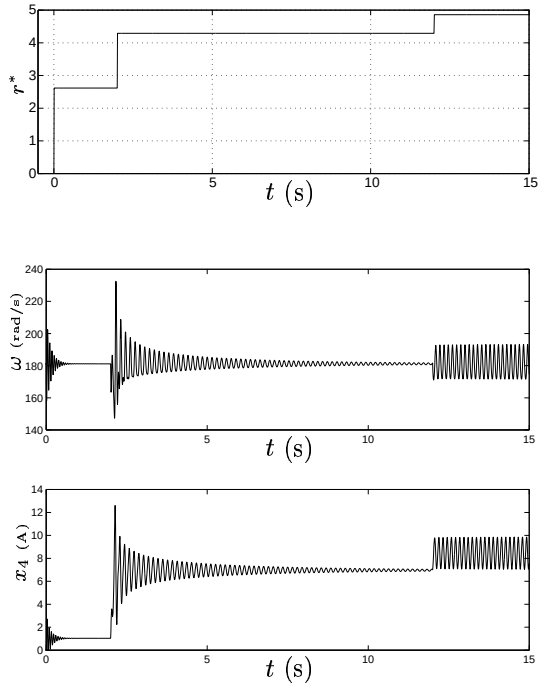

Figure 6. Speed and quadrature axis current for load torque variations; $\kappa = 2.7$, $\lambda_{1,2} = (-1.2 \pm j7)c_1$.

References

Bazanella, A. and Reginatto, R. (2000). Robustness margins for indirect field oriented control of induction motors, *IEEE Trans. Aut. Cont.* **45**(6): 1226–1231.

Bazanella, A., Reginatto, R. and Valiati, R. (1999). On hopf bifurcations in indirect field oriented control of induction motors: designing a robust PI controller, *Conference on Decision and Control*, Phoenix, Arizona.

Bazanella, A. S. and Reginatto, R. (2001). Robust tuning of the speed loop in indirect field oriented control of induction motors - to appear, *Automatica* .

Bazanella, A. S., Reginatto, R. and Valiatti, R. (2000). Robustness margins for global asymptotic stability in indirect field-oriented control of induction motors, *XIII Congresso Brasileiro de Automática*, Florianópolis, Brasil, pp. 1048–1053.

Bose, B. (1987). *Power Electronics and AC Drives*, Prentice-Hall, Englewood Cliffs, New Jersey.

De Wit, P., Ortega, R. and Mareels, I. (1996). Indirect field-oriented control of induction motors is robustly globally stable, *Automatica* **32**(10): 1393–1402.

Espinosa-Perez, G., Chang, G., Ortega, R. and Mendes, E. (1998). On field-oriented control of induction motors: Tuning of the PI gains for performance enhancement, *Conference on Decision and Control*, Tampa, Florida, pp. WM15–2.

Krishnan, R. and Doran, F. C. (1987). Study of parameter sensitivity in high-performance inverter-fed induction motor drive systems, *IEEE Trans. Ind. Applic.* **IA-23**(4): 623–635.

Leonhard, W. (1985). *Control of Electrical Drives*, Springer-Verlag, Berlin.

Marino, R., Peresada, S. and Valigi, P. (1993). Adaptive input-output linearizing control of induction motor, *IEEE Trans. Aut. Cont.* **38**(2): 208–221.

Novotny, D. and Lorenz, R. (1986). *Introduction to Field Orientation and High Performance AC Drives*, IEEE.

Ortega, R., Nicklasson, P. and Péres, G. (1996). On speed control of induction motors, *Automatica* **32**(3): 455–460.

Reginatto, R. and Bazanella, A. S. (2000). Robustness of global asymptotic stability in indirect field-oriented control of induction motors, *Conference on Decision and Control*, Sydney, Australia.